

innovative techniques

A single-breath technique with variable flow rate to characterize nitric oxide exchange dynamics in the lungs

NIKOLAOS M. TSOUKIAS,¹ HYE-WON SHIN,¹ ARCHIE F. WILSON,² AND STEVEN C. GEORGE^{1,3}

¹Department of Chemical and Biochemical Engineering and Materials Science, ²Center for Biomedical Engineering, Department of Medicine, and ³Division of Pulmonary and Critical Care, University of California, Irvine, California 92697

Received 21 November 2000; accepted in final form 12 March 2001

Tsoukias, Nikolaos M., Hye-Won Shin, Archie F. Wilson, and Steven C. George. A single-breath technique with variable flow rate to characterize nitric oxide exchange dynamics in the lungs. *J Appl Physiol* 91: 477–487, 2001.—Current techniques to estimate nitric oxide (NO) production and elimination in the lungs are inherently nonspecific or are cumbersome to perform (multiple-breathing maneuvers). We present a new technique capable of estimating key flow-independent parameters characteristic of NO exchange in the lungs: 1) the steady-state alveolar concentration ($C_{\text{alv,ss}}$), 2) the maximum flux of NO from the airways ($J_{\text{NO,max}}$), and 3) the diffusing capacity of NO in the airways ($D_{\text{NO,air}}$). Importantly, the parameters were estimated from a single experimental single-exhalation maneuver that consisted of a preexpiratory breath hold, followed by an exhalation in which the flow rate progressively decreased. The mean values for $J_{\text{NO,max}}$, $D_{\text{NO,air}}$, and $C_{\text{alv,ss}}$ do not depend on breath-hold time and range from 280–600 pl/s, 3.7–7.1 pl·s⁻¹·parts per billion (ppb)⁻¹, and 0.73–2.2 ppb, respectively, in two healthy human subjects. A priori estimates of the parameter confidence intervals demonstrate that a breath hold no longer than 20 s may be adequate and that $J_{\text{NO,max}}$ can be estimated with the smallest uncertainty and $D_{\text{NO,air}}$ with the largest, which is consistent with theoretical predictions. We conclude that our new technique can be used to characterize flow-independent NO exchange parameters from a single experimental single-exhalation breathing maneuver.

parameter estimation; diffusing capacity; airways; inflammation

THE CONCENTRATION OF NITRIC oxide (NO) that appears in the exhaled breath depends strongly on several factors, including the presence of inflammation (1, 9). The fact that inflammatory diseases, such as bronchial asthma, elevate exhaled NO has generated great interest in

using exhaled NO as a noninvasive index of pulmonary inflammation (2). Unfortunately, many early reports collected NO levels under different experimental conditions, and the absolute concentrations, as well as the conclusions, were not consistent. Subsequent work demonstrated that the exhaled NO level also depends on many additional factors, including the exhalation flow rate and the position of the soft palate (which affects nasal cavity contribution) (10, 15). These findings generated formal recommendations by both the American Thoracic Society (ATS) and the European Respiratory Society (ERS) on the conditions under which exhaled NO should be collected (8, 17). Both reports recommend a constant exhalation flow rate during the maneuver (ERS recommends 250 ml/s, the ATS recommends 50 ml/s).

Recently, several groups have demonstrated that exhaled NO arises from both the alveolar and airway regions of the lungs (12, 16, 19, 20); this conclusion is supported by the presence of nitric oxide synthase (NOS) in cells present in both regions (6, 13, 18, 21). The flow rate dependence is due to the source of NO in the airways, and this finding prompted the recommendation of a single constant flow rate in all experimental protocols. However, this recommendation presents a critical limitation in the interpretation of the exhaled NO. Namely, the constant flow rate maneuver cannot provide information regarding the origin of the endogenous NO production (i.e., the relative contribution from the airways and the alveoli). As a result, a single exhalation with a constant exhalation flow rate is inherently nonspecific, since two subjects can potentially have the same exhaled NO concentration yet have different relative contributions from the airways and alveoli. For example, two subjects with different in-

Address for reprint requests and other correspondence: S. C. George, Dept. of Chemical and Biochemical Engineering and Materials Science, 916 Engineering Tower, Univ. of California, Irvine, CA 92697-2575 (E-mail: scgeorge@uci.edu).

The costs of publication of this article were defrayed in part by the payment of page charges. The article must therefore be hereby marked "advertisement" in accordance with 18 U.S.C. Section 1734 solely to indicate this fact.

flammatory diseases (i.e., asthma and interstitial pneumonia) could have identical exhaled NO levels at a constant exhalation flow. The exhaled NO from the patient with asthma would largely arise from the airways, whereas the exhaled NO from the patient with allergic alveolitis (11) (alveolar inflammation) would largely arise from the alveolar region. However, by using only the exhaled concentration at a single expiratory flow as an index, the diseases could not be distinguished.

To avoid this problem, we have previously presented a technique that utilized multiple single-exhalation maneuvers at different constant exhalation flow rates as a means of separately determining airway and alveolar contributions (19, 20). The airway contribution was characterized by the flux from the airway wall (mol NO/s or ml NO/s) and the alveolar contribution by the steady-state alveolar concentration (parts per billion; ppb). Recently, two research groups reported an alternative technique in which the flux from the airway compartment was characterized by two terms: the airway diffusing capacity and either the airway wall concentration (16) or the maximum rate of production of NO by the airways that enters the airstream (maximum flux of NO from the airways) (12, 16). This was achieved by utilizing very low constant expiratory flow rate maneuvers. All of the previous techniques require multiple single exhalations, and the accuracy (or confidence level) of the estimated parameters is positively correlated with the number of single exhalations utilized. Multiple breathing maneuvers are cumbersome and time consuming. Furthermore, constant flow rate maneuvers can be difficult to perform, especially at very low flows and by young subjects.

The goal of this study is to present a new technique to characterize NO exchange parameters. The method involves an appropriate analysis of an individual (i.e., not multiple) single-exhalation maneuver with a variable flow rate. The technique allows 1) estimation of flow-independent parameters characteristic of NO exchange dynamics from a single maneuver and 2) prediction of the plateau NO concentration at a constant exhalation flow rate. The new method of analysis is more versatile because it provides a means to analyze exhaled NO data when flow rate is not necessarily constant. Furthermore, by inducing specific changes in flow rate during a single exhalation, the technique renders a single-exhalation maneuver sufficient to acquire all the necessary information. The focus of this manuscript is to describe the theory underlying the technique, test the technique in two normal subjects (one experienced and one naive to breathing maneuvers), and characterize the intrinsic intramaneuver and intrasubject variability, in particular, the effect of breath-hold time on the variability of the estimated parameters.

Glossary

C_{air} Concentration (ppb) of NO in the airway compartment

$C_{\text{alv,ss}}$	Steady-state alveolar concentration of NO (ppb)
C_{exh}	Exhaled concentration (ppb)
C_{exh}^*	Model-predicted exhaled concentration (ppb)
C_I	Inspired concentration (ppb)
$\bar{C}_{\text{tiss,air}}$	Mean (over radial position) concentration of NO within the tissue phase (ppb)
$D_{\text{NO,air}}$	Diffusing capacity ($\text{ml}\cdot\text{s}^{-1}\cdot\text{ppb}^{-1}$) of NO in the airways
F	F statistic test
$\Delta\bar{I}_{1-\alpha,i}^m$	Intramaneuver $100(1 - \alpha)\%$ confidence interval
$\Delta\bar{I}_{1-\alpha,i}^s$	Intrasubject $100(1 - \alpha)\%$ confidence interval
J_{NO}	Volumetric flux per unit airway volume ($\text{ml}\cdot\text{s}^{-1}\cdot\text{ml}^{-1} = \text{ppb/s} \times 10^{-9}$) of NO
$J_{\text{NO,max}}$	Maximum total molar flux (ml/s) of NO from the airway wall
n	Number of data points
\mathbf{P}	Covariance matrix
S^{sr}	Semi-relative sensitivity index
t_{DS}	Convective transport delay time in the dead space volume
τ_{res}	Residence time of each differential gas bolus in the airway compartment
V	Axial (or longitudinal) position from the distal region of the airway to the mouth (units of cumulative volume)
V_{air}	Volume of the airway compartment (ml)
VC	Vital capacity (ml)
V_{DS}	Dead space volume (volume expired before observation of NO signal) (ml)
\dot{V}_E	Volumetric flow rate of air during expiration
\dot{V}_I	Volumetric flow rate of air during inspiration
\mathbf{Y}_{LS}	$100(1 - \alpha)\%$ confidence region for the vector of inputs

METHODS

Two-compartment model. A simple two-compartment mathematical model has been previously developed to describe the exchange dynamics of NO in the human lungs (19). We will utilize the governing equations of this model in our parameter estimation algorithm and will review only the salient features here. The model is summarized pictorially in Fig. 1 and consists of a rigid tubular compartment representing the airways (trachea-airway generation 17) and a well-mixed expansile compartment representing the alveoli (airway generation 18 and beyond). A tissue layer representing the bronchial mucosa surrounds the airway. Exterior to the tissue is a layer of blood representing the bronchial circulation and serves as an infinite sink for NO (i.e., zero concentration of NO).

The axial gas-phase transport is characterized by bulk convection (advection). The tissue phase produces NO uniformly, and at a constant rate, and consumes NO in a first-order fashion. The outer boundary of the tissue is assumed to be blood. Because the reaction of NO with hemoglobin within the red blood cell is very rapid and there are abundant protein thiols (e.g., albumin) in plasma, the concentration of free NO in the blood is assumed to be zero. Transport between the tissue and gas phase is described with Fick's first

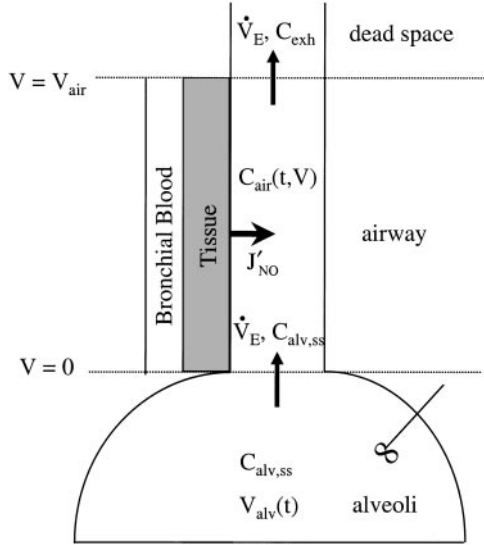


Fig. 1. Schematic of two-compartment model used to describe nitric oxide (NO) exchange dynamics. The alveolar compartment has been simplified to represent only the steady-state concentration during exhalation. Parameters are described in the text.

law of diffusion. The concentration profile in the tissue has been shown to rapidly (< 0.6 s) reach a steady state (19); thus the mass balance in the airway compartment retains an analytical solution. The second compartment represents the alveolar regions of the lungs and is thus expansible and considered to have a uniform concentration spatially. The model is meant to simulate the oral exhalation profile and thus assumes that there is no nasal contribution to exhaled NO.

We, as well as other researchers, have previously demonstrated that alveolar concentration reaches a steady-state concentration in < 10 s following inspiration (7, 19). Thus, in the development of our current technique, we have simplified the alveolar compartment and will characterize the alveolar region by the steady-state alveolar concentration, $C_{alv,ss}$. This simplification is justified for inspiration of NO-free air and for exhalation following at least a 10-s breath hold.

A mass balance in the airway compartment produces the following differential equation

$$\frac{\partial C_{air}}{\partial t} = -\dot{V} \frac{\partial C_{air}}{\partial V} + J'_{NO} \quad (1)$$

where J'_{NO} is the volumetric flux per unit airway volume ($\text{ml} \cdot \text{s}^{-1} \cdot \text{ml}^{-1} = \text{ppb/s} \times 10^{-9}$) of NO between the tissue and gas phases in the airway compartment and depends on C_{air} and \dot{V} is volumetric flow rate of air (negative during \dot{V}_I and positive during \dot{V}_E), which can depend on time.

Flux of NO from airway wall. A previously described description of the exchange dynamics in the airway tissue layer, which incorporates endogenous production, reaction, and diffusion, predicts J'_{NO} to be a linear function of the bulk gas concentration (19). In agreement with earlier works (12, 16, 19), we assume a uniform distribution for J'_{NO} along the airway tree (i.e., the same linear dependence between J'_{NO} and C_{air} holds throughout the airways). The following linear relationship between J'_{NO} and C_{air} then holds (19)

$$J'_{NO} = \left(\frac{J_{NO,max}}{V_{air}} \right) - \left(\frac{D_{NO,air}}{V_{air}} \right) \times C_{air} \quad (2)$$

Thus we will characterize J'_{NO} with two parameters: $J_{NO,max}$ and $D_{NO,air}$.

Model solution. Assuming a spatially uniform distribution of J'_{NO} , the solution for C_{exh} , which follows from Eqs. 1 and 2, has the following form

$$C_{exh}(t + t_{ds}) = C_{air}(t, V = V_{air}) = \left(C_{in}(t - \tau_{res}) - \frac{J_{NO,max}}{D_{NO,air}} \right) e^{-\frac{D_{NO,air}}{V_{air}} \tau_{res}(t)} + \frac{J_{NO,max}}{D_{NO,air}} \quad (3)$$

where C_{in} is the inlet concentration to the airway compartment. We can distinguish two different cases

$$\text{Case I (phases I and II of exhalation):} \int_{t - \tau_{res}(t)}^{t + t_{ds}} \dot{V}(t') dt' = 0 \quad (4)$$

$$\text{Case II (phase III of exhalation):} \int_{t - \tau_{res}(t)}^{t + t_{ds}} \dot{V}_E(t') dt' = V_{air} + V_{DS} \quad (5)$$

Case I represents the emptying of the gas in phases I and II of the exhalation profile (see below). This exhaled gas consists of the inspired gas that has resided only in the airway compartment and has not reached the alveoli. For this case, C_{in} is simply C_I ($C_I = 0$ by ATS guidelines) and $\tau_{res}(t)$ is calculated from Eq. 4. In other words, the net volume transpired by each bolus is zero and is given by the integral of the flow rate over the time period of interest. The flow signal during this time period would include inspiration (negative flow rate), breath hold (zero flow rate), and expiration (positive flow rate).

Case II represents the emptying of the gas in phase III of the exhalation profile or the alveolar plateau. Phase II is not described by the model because axial diffusion is neglected to preserve an analytical solution; the compensation for this simplification is described below in *Parameter estimation*. During phase III, the expired air originates primarily from the alveolar compartment. Thus C_{in} is equivalent to $C_{alv,ss}$, and $\tau_{res}(t)$ is calculated from Eq. 5. In this case, the flow signal is provided entirely by the expiratory flow rate.

Figure 2 depicts a schematic of the method used for analyzing the experimental data (Eqs. 3–5). The flow and NO signal were first synchronized to account for the delay of the NO analyzer relative to the flowmeter. Then, for a bolus of gas that reaches the sampling port of the analyzer at time $t + t_{ds}$, t_{ds} and τ_{res} can be estimated using backward integration of the expiratory flow signal if V_{DS} and V_{air} are known. V_{DS} is approximated from the volume the subject needs to expire

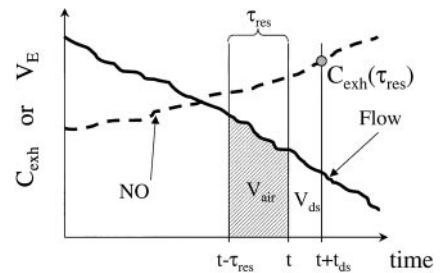


Fig. 2. Schematic demonstrating the “backward” integration of the flow signal to convert exhalation time to residence time of each exhaled bolus of gas. The concentration of a gas bolus is determined at time $t + t_{ds}$. By using the flow rate history of the bolus, one can integrate the flow rate signal backward until the volume of the dead space and the airway volume have been traversed. In doing so, one can determine the residence time in the airway compartment. Mathematical details are presented in the text.

before a change in C_{exh} is observed (after the signals have been synchronized). A first approximation of V_{air} will be the physiological dead space in milliliters, as approximated by the weight (assuming normal body fat) of the subject in pounds plus the age of the subject in years (5). During the backward integration, each exhaled bolus is treated according to *case I or II*, depending on which condition of *Eqs. 4 and 5* is satisfied. *Equation 3* can be used to simulate the experimental profiles.

Equations 3–5 allow analysis of a single exhalation with a variable flow rate. Together, the equations simply state that, in the absence of interaction between neighboring differential boluses of gas (i.e., no axial diffusion) and for a uniformly distributed J_{NO} , $C_{\text{exh}}(t)$ will depend on only five unknown parameters: $C_{\text{alv,ss}}$, $D_{\text{NO,air}}$, $J_{\text{NO,max}}$, V_{air} , and $\tau_{\text{res}}(t)$. If one has a previous estimate of V_{air} , one can then determine $\tau_{\text{res}}(t)$ from *Eqs. 4 and 5*, and the problem is reduced to estimating three flow-independent parameters ($C_{\text{alv,ss}}$, $D_{\text{NO,air}}$, $J_{\text{NO,max}}$) from C_{exh} as a function of $\tau_{\text{res}}(t)$.

Sensitivity analysis. We define the semirelative sensitivity of C_{exh} with respect to the unknown parameters in the following fashion

$$S_i^{\text{sr}} = Y_i \frac{\partial C_{\text{exh}}}{\partial Y_i} \quad (6)$$

where Y is one of the unknown parameters and the subscript “ i ” represents the specific parameter. The derivatives are estimated at the nominal values of each parameter. S^{sr} represents the absolute change of C_{exh} per fractional change of the corresponding parameter and is useful for 1) providing a useful relative index of comparison between the unknown parameters and their impact on C_{exh} and 2) determining the confidence region of the estimated parameters. The partial derivatives can be calculated analytically by differentiation of *Eq. 2* with respect to the corresponding variable. A necessary condition for an accurate estimation of the parameters of interest is that the model’s output should be sensitive enough relative to the intrinsic error of the experimental measurement.

In Fig. 3, we plot S^{sr} as a function of τ_{res} . It is clear that C_{exh} is quite sensitive to $J_{\text{NO,max}}$ and $C_{\text{alv,ss}}$; however, $S_{\text{sr}}^{D_{\text{NO,air}}}$ is high only for high τ_{res} . The analysis suggests that residence times >10 s are required to achieve a similar sensitivity index (and thus confidence in the estimate) as that obtained for $J_{\text{NO,max}}$ and $C_{\text{alv,ss}}$ at a residence of time of ~ 1 s. This is consistent with the need to utilize very small flow

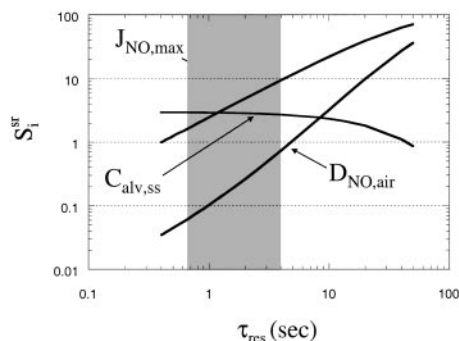


Fig. 3. Semirelative sensitivity of C_{exh} to the 3 input parameters. The shaded region represents the range of airway compartment residence times achieved during a decreasing flow rate maneuver that spans an exhalation flow rate of 300 to 50 ml/s for an airway compartment volume of 200 ml.

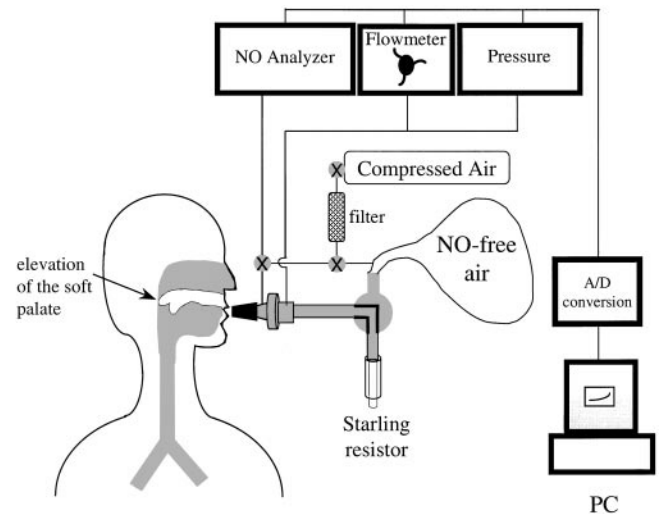


Fig. 4. Schematic of the experimental setup used to collect the exhalation profiles. The flow, pressure, and NO analog signals are captured by the analytical instruments and converted to a digital signal. A series of valves allows NO-free air to be stored in a Mylar bag for inspiration. During the breath hold, the NO analyzer samples from the NO-free air reservoir and the subject maintains a positive pressure of >5 cmH₂O by attempting to exhale against a closed valve. As exhalation begins, the NO analyzer then samples from the exhalate and the flow rate is manipulated by a variable Starling resistor while the expiratory effort of the subject remains constant.

rates (<10 ml/s) in previous attempts to estimate $D_{\text{NO,air}}$ (12, 16). In practice, we found that it is difficult to perform such a maneuver, especially by young subjects, and accurately record such low flow rates. Alternatively, we will utilize a preexpiratory breath hold to produce large enough residence times to accurately estimate $D_{\text{NO,air}}$.

Experimental protocol. A series of single exhalation maneuvers were performed on two subjects, one experienced and one naive to performing breathing maneuvers, to determine the feasibility of the new technique. The protocol was approved by the Institutional Review Board at the University of California, Irvine, and the schematic is shown in Fig. 4. The first subject was a healthy male, age 28 yr, body weight 172 lb., vital capacity 5,000 ml, an author on this manuscript (Tsoukias), and experienced at performing breathing maneuvers. The second subject was a healthy male, age 23 yr, body weight 175 lb., and vital capacity 5,200 ml but was not experienced at performing breathing maneuvers. The anatomic airway volume was thus estimated to be 200 ml and 198 ml for the two subjects, respectively (5).

The subjects performed a series of single oral exhalation breathing maneuvers against a small resistance (>5 cmH₂O) for the isolation of the nasal cavity (17). The subjects first performed vital capacity maneuvers at a constant exhalation flow of ~ 50 ml/s and ~ 250 ml/s as described by the ATS and ERS guidelines to determine the plateau concentration of NO. A constant flow was facilitated by a Starling resistor (Hans-Rudolph, Kansas City, MO) in which the resistance could be altered to achieve the desired flow rate. The subjects then performed a series of single exhalations after a period of breath holding. The period of breath holding was either 10, 20, 30, or 45 s, and each maneuver was repeated five times. During the breath hold, the subject exerted an expiratory effort against a closed valve to maintain a positive pressure of >5 cmH₂O, and the NO sampling line sampled air from

the zero NO reservoir. Then, just before exhalation, a valve on the NO sampling line was changed to sample from the exhaled breath and the exhalation valve was opened, allowing the patient to expire. The expiratory flow rate progressively decreased during the exhalation from an initial value of ~ 300 ml/s ($\sim 6\%$ of the vital capacity per second) to ~ 50 ml/s ($\sim 1\%$ of the vital capacity per second), and a positive pressure >5 cmH₂O was maintained. To facilitate such a flow rate pattern, the expiratory resistance was altered throughout the maneuver while the subject was instructed not to change the expiratory effort. By monitoring online the flow signal and by progressively increasing the resistance, we were able to produce the desired flow rate pattern.

An exponentially decreasing flow rate with volume that ranges from $\sim 6\%$ of the vital capacity per second to $\sim 1\%$ of the vital capacity per second was set as a target (see APPENDIX), although this is not required. This choice satisfies two basic requirements for the flow rate pattern: 1) a uniform residence time distribution of the exhaled gas in the airways and 2) minimal acceleration of a single bolus of gas inside the airways (see DISCUSSION and APPENDIX).

NO concentration was measured using a chemiluminescence NO analyzer (NOA280, Sievers, Boulder, CO). An operating reaction cell pressure was maintained at 7.5 Torr, which provided a sampling flow rate of 250 ml/min (Fig. 4). The instrument was calibrated on a daily basis using a certified NO gas (25 ppm in N₂, INO max Sensor-medics). The zero point calibration was performed with an NO filter (Sievers). Due to a small drift in the calibration of the instrument during the day, we performed zero point calibration immediately before the collection of a profile. The flow rate was measured using a pneumotachometer (RSS100, Hans-Rudolph). The pneumotachometer was calibrated daily and was set to provide the flow in units of STPD. The analog signals of flow and NO were digitized using an A/D card at a rate of 50 Hz and stored on a personal computer for further analysis.

Parameter estimation. Identification of the unknown parameters ($C_{alv,ss}$, $D_{NO,air}$, $J_{NO,max}$) is accomplished by nonlinear least-square minimization. Assuming a constant variance error in the measurement renders ordinary least squares sufficient for parameter estimation. Least square minimization of the sum of the residuals (R_{LS}) between the model's prediction and the experimental data was accomplished with the use of a conjugated direction minimization algorithm.

Figure 5 presents a representative exhalation profile from *subject 1* simulated by the model. The model does not precisely predict phases I and II of the exhalation profile, in which the accumulated NO during breath holding in the conducting airways and transition region of the lungs exits the mouth. This discrepancy is attributed to axial diffusion that our model neglects. Although the precise shape of phase I cannot be accurately simulated with the model, the absolute amount of NO in phases I and II can be predicted. Thus our technique utilizes the information from phases I and II (where τ_{res} is large and hence the sensitivity to $D_{NO,air}$ is high) by forcing the model to simulate the total amount of NO exiting in phases I and II of the exhalation in addition to simulating the precise C_{exh} over phase III. Thus the fitting of the experimental data will include minimization of the sum of two terms: 1) the squared residual in the average concentrations in phases I and II weighted by the number of data points and 2) the sum of the squared residual of C_{exh} in phase

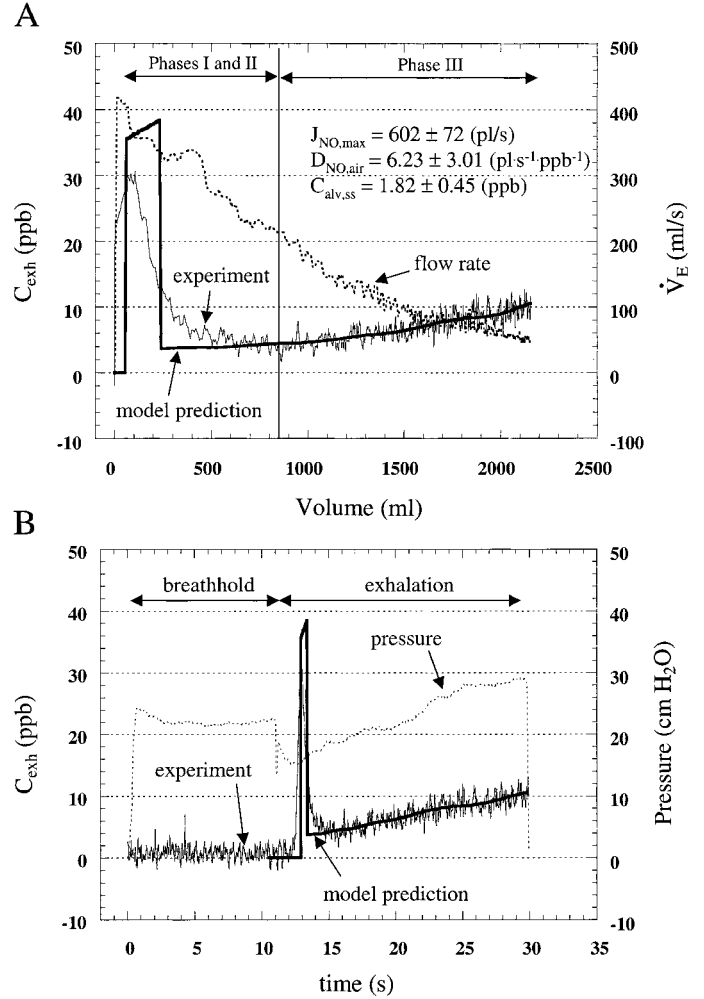


Fig. 5. Representative exhaled NO concentration profile following a 20-s breath hold shown as a function of exhaled volume (A) or time (B). The light line represents exhaled NO concentration (parts/billion; ppb), and the dashed line represents the exhalation flow rate (A) or pressure (B). The heavy line represents the best-fit model prediction of the exhalation curve using nonlinear least squares regression. The optimal values for 3 unknown input parameters ($C_{alv,ss}$, $D_{NO,air}$, and $J_{NO,max}$) are shown for this particular maneuver. Parameters and mathematical details are presented in the text.

III of the exhalation profile according to the following relationship

$$R_{LS} = n_{I,II} \cdot \left[\frac{\sum_{i=1}^{n_{I,II}} C_{exh,i}^* \cdot \Delta V_{I,II}}{V_{I,II}} - \frac{\sum_{i=1}^{n_{I,II}} C_{exh,i} \cdot \Delta V_{I,II}}{V_{I,II}} \right]^2 + \sum_{i=1}^{n_{III}} (C_{exh,i}^* - C_{exh,i})^2 \quad (7)$$

where $n_{I,II}$ and $V_{I,II}$ are the number of data points and volume in phases I and II, n_{III} and V_{III} are the number of data points and volume in phase III, and $\Delta V_{I,II}$ is the change in volume between consecutive data points ($\dot{V}_E \times dt$). To ensure complete emptying of the airway compartment following breath hold, we define the transition from phases II and III as the point in the exhalation for which the slope (dC_{exh}/dV) of the exhalation profile is zero.

Identifiability and uncertainty analysis. A high sensitivity is a necessary but not sufficient condition for an accurate estimation of the parameters. Dependence between the parameters may render them unidentifiable even when their sensitivities are significant. Thus, although the sensitivity analysis suggests experimental conditions for improving the estimation of the parameters, a better index is needed to describe the accuracy of our estimation.

Once the matrix \mathbf{X} of the sensitivity coefficients at every t_i can be estimated [i.e., $\mathbf{X}_{i,j} = S_i^{r(t_j)}$], a confidence region for the estimated parameters can be acquired from the variance-covariance matrix of the estimation (3). Assuming additive zero mean and normally distributed measurement errors and errorless measured inputs, the $100(1 - \alpha)\%$ confidence region for the ordinary least square estimation of the vector of inputs, \mathbf{Y}_{LS} , is approximated from

$$(\mathbf{Y}_{LS} - \beta)^T \mathbf{P}^{-1} (\mathbf{Y}_{LS} - \beta) = p F_{1-\alpha}(p, n - p) \quad (8)$$

where β is their expected true value, superscript T denotes transpose, and $F_{1-\alpha}$ is the F statistic test for the number of estimated parameters, p , (i.e., 3 in our case), and the number of data points, n . For an ordinary least square estimation with the additional assumption of constant variance, and uncorrelated errors, the covariance matrix \mathbf{P} is

$$\mathbf{P} = (\mathbf{X}^T \mathbf{X})^{-1} \sigma^2 \quad (9)$$

and an unbiased estimation of the constant variance σ^2 is given by

$$s^2 = E(\sigma^2) = R_{LS}/(n - p). \quad (10)$$

The approximate confidence regions are the interior of the hyperellipsoids provided by Eq. 9. The maximum range of the parameters in these contours can be estimated from the eigenvalues of \mathbf{P} as follows

$$\Delta \bar{\mathbf{I}}_{1-\alpha,i}^m = (\pm p F_{1-\alpha}(p, n - p) e_1(\lambda_1)^{-1/2})_{i-\text{row}} / \mathbf{Y}_i \quad (11)$$

where λ_1 is the smaller eigenvalue of the \mathbf{P} matrix and e_1 is the corresponding eigenvector (3). Thus $\Delta \bar{\mathbf{I}}_{1-\alpha,i}^m$ provides the normalized (by the estimated value of parameter i) confidence region of the estimated parameters for a single maneuver or an intramaneuver confidence interval.

We can also define a normalized intrasubject (intermaneuver) confidence interval by using the standard deviation (SD) of the estimate of each of the parameters for the five repeated maneuvers

$$\Delta \bar{\mathbf{I}}_{1-\alpha,i}^s = \pm \frac{\text{SD}}{\sqrt{n_m}} t_{1-\alpha} / \mathbf{Y}_i \quad (12)$$

where n_m is the number of breathing maneuvers and $t_{1-\alpha}$ is the critical t -value for $n_m - 1$ degrees of freedom.

RESULTS

Figure 6 presents the estimated parameters ($J_{\text{NO,max}}$, $D_{\text{NO,air}}$, and $C_{\text{alv,ss}}$, respectively) for each of the five repeated breathing maneuvers (four maneuvers for a 45-s breath hold) for both subjects (*subject 1* is shown on *left*). The mean estimated value with error bars representing the mean $\Delta \bar{\mathbf{I}}_{0.95,i}^m$ (Eq. 11) is also shown. That is, for each maneuver, an independent estimate of the confidence region is estimated from Eq. 11, and the error bar represents the mean of these intramaneuver confidence region estimates. Figure 6 also shows the mean estimated value, with error bars representing

the mean $\Delta \bar{\mathbf{I}}_{0.95,i}^s$ (Eq. 12, or intrasubject variability). The mean values for $J_{\text{NO,max}}$, $D_{\text{NO,air}}$, and $C_{\text{alv,ss}}$ do not depend on breath-hold time and range from 580 to 600 pl/s, 4.6 to 7.1 pl·s⁻¹·ppb⁻¹, and 1.8 to 2.2 ppb for *subject 1* and 280 to 440 pl/s, 3.7 to 4.1 pl·s⁻¹·ppb⁻¹, and 0.73 to 1.5 ppb for *subject 2*. These values compare favorably with those previously reported by our group (19, 20), Pietropaoli et al. (12), and Silkoff et al. (16) using techniques that require multiple-breathing maneuvers.

The intramaneuver estimate of $J_{\text{NO,max}}$ steadily improves (as evidenced by a decreasing confidence interval) as the breath-hold time increases from 10 to 30 s. The mean $\Delta \bar{\mathbf{I}}_{0.95,i}^m$ is 17 and 89% for *subjects 1* and 2, respectively, at a 10-s breath hold and decreases to 6.5 and 19%, respectively, for a 30-s breath hold. No significant improvement is seen with a 45-s breath hold. The same trend is observed for $D_{\text{NO,air}}$ except the magnitude of the uncertainty is larger. The mean $\Delta \bar{\mathbf{I}}_{0.95,C_{\text{alv,ss}}}^m$ is 89 and 941% for *subjects 1* and 2, respectively, at a 10-s breath hold and decreases to 19 and 159%, respectively, for a 30-s breath hold.

A similar, although more modest, trend with breath-hold time is observed for $C_{\text{alv,ss}}$. The mean $\Delta \bar{\mathbf{I}}_{0.95,C_{\text{alv,ss}}}^m$ improves by increasing the breath-hold time from 10 to 20 s (34 and 280% to 26 and 78% for *subjects 1* and 2, respectively) but then remains nearly constant for breath-hold times >20 s. Importantly, there is no statistical difference between the estimated values for any of the parameters at different breath-hold times, only a change in the estimated confidence interval.

The intrasubject estimate of the three parameters consistently improves (as evidenced by a decreasing confidence interval) as the breath-hold time increases from 10 to 20 s with modest or no significant improvement for breath-hold times >20 s. The mean $\Delta \bar{\mathbf{I}}_{0.95,J_{\text{NO,max}}}^m$ is 25 and 41% for *subjects 1* and 2 at a 10-s breath hold that decreases to 13 and 8.3% for a 20-s breath hold, respectively. The mean $\Delta \bar{\mathbf{I}}_{0.95,D_{\text{NO,air}}}^m$ is 114 and 90% for *subjects 1* and 2, respectively, for a 10-s breath hold and decreases to 45 and 32%, respectively, for a 20-s breath hold. For $C_{\text{alv,ss}}$, the mean $\Delta \bar{\mathbf{I}}_{0.95,C_{\text{alv,ss}}}^m$ is 47 and 63% for *subjects 1* and 2, respectively, for a 10-s breath hold and decreases to 28 and 24%, respectively, for a 20-s breath hold.

In general, the mean value for $\Delta \bar{\mathbf{I}}_{0.95,i}^m$ differs from the mean value of $\Delta \bar{\mathbf{I}}_{0.95,i}^s$ because $\Delta \bar{\mathbf{I}}_{0.95,i}^m$ depends inversely on the square root of the number of maneuvers performed (Eq. 12) and on the reproducibility of the experimental conditions and measurements. In addition, it is also of interest to note that the intramaneuver confidence intervals for *subject 1* are much smaller than for *subject 2*, yet the intrasubject confidence intervals are, in general, larger.

In Fig. 7, NO plateau concentration ($C_{\text{exh,ee}}$, concentration at end exhalation) from a constant exhalation flow rate is plotted as a function of \dot{V}_E . The model prediction (solid line) is calculated using the mean estimated parameters from the five repeated 20-s breath-hold maneuvers. Mean $C_{\text{exh,ee}}$ values ($\pm 95\%$ confidence interval) from the experimental maneuvers with the recommended (8, 17) constant flow rates are

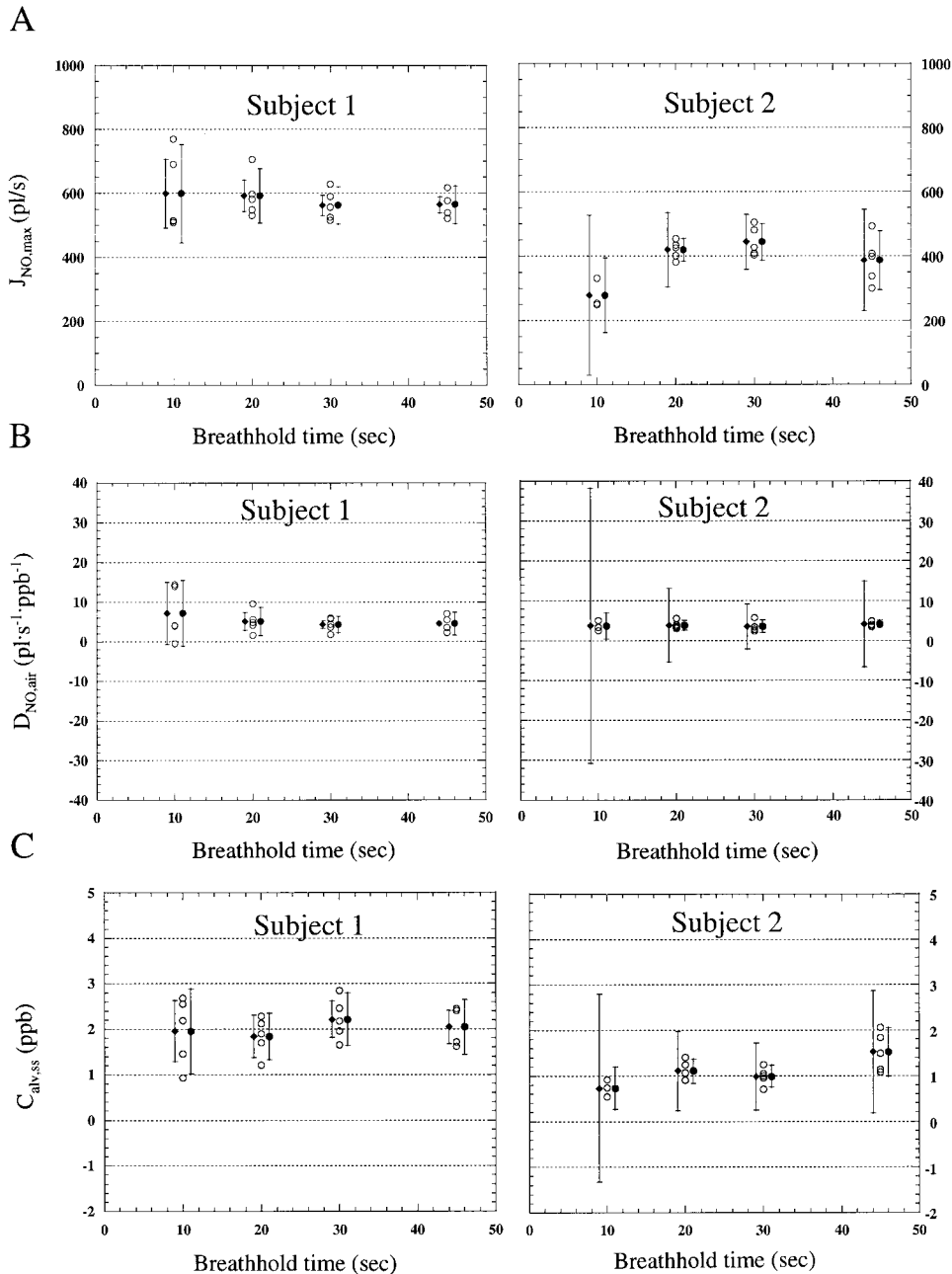


Fig. 6. Optimal parameter values for $J_{NO,max}$ (A), $D_{NO,air}$ (B), and $C_{alv,ss}$ (C) following 5 repeated decreasing flow rate exhalation breathing maneuvers (○) following 4 different breath-hold times (10, 20, 30, and 45 s) for 2 subjects. *Subject 1* (left) was experienced at performing breathing maneuvers, and *subject 2* (right) was naive. ♦, Mean optimal parameter value; error bars are the mean intramanuever 95% confidence intervals. ●, Mean optimal parameter value; error bars are the mean intrasubject 95% confidence intervals.

also presented. The predicted NO plateau concentrations are in close agreement with the experimental measurements. Importantly, this figure demonstrates that, once the unknown flow-independent parameters have been estimated, the model can be utilized to accurately predict the NO plateau concentration, at least for constant flow rates between 50 and 300 ml/s.

In Fig. 8, the effect of V_{air} in the estimation of the unknown parameters of interest is investigated. The 20-, 30-, and 45-s breath-hold maneuvers were reanalyzed for *subject 1* with two smaller values for V_{air} (100 and 150 ml) instead of the control value of 200 ml. There is a statistically significant difference in the estimation of all three parameters ($P < 0.01$) with decreasing V_{air} at each breath-hold time. There is a positive correlation between the estimated values of

$J_{NO,max}$ and $D_{NO,air}$ with V_{air} and a negative correlation for $C_{alv,ss}$. The percent change in the estimated parameters per milliliter change in V_{air} has averaged values of 0.2, 1.5, and -0.3% for $J_{NO,max}$, $D_{NO,air}$, and $C_{alv,ss}$, respectively.

DISCUSSION

In this manuscript, we present a new method for the analysis and interpretation of exhaled NO data. This new technique can estimate three flow-independent parameters ($J_{NO,max}$, $D_{NO,air}$, and $C_{alv,ss}$) from a single-exhalation maneuver that can comprehensively characterize the exhalation NO profile. The technique requires only a single-breathing maneuver and is therefore less cumbersome to perform than other tech-

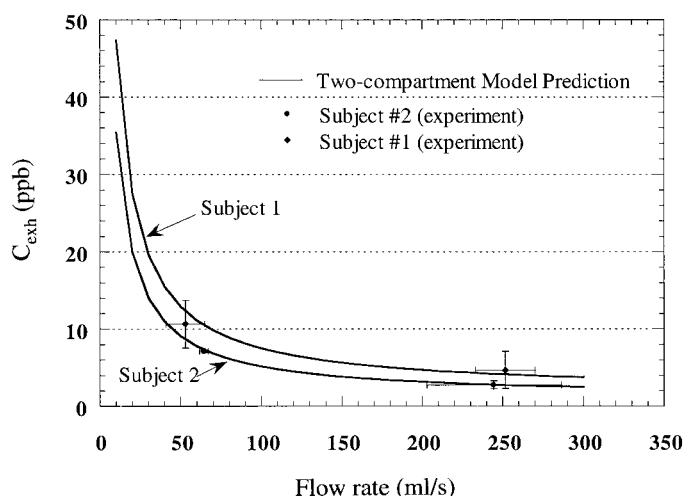


Fig. 7. C_{exh} at end exhalation is shown as a function of the constant exhalation flow rate for both subjects. Error bars in the experimental data points represent 95% confidence intervals. Two exhalation flow rates are shown (~ 50 and ~ 250 ml/s) based on American Thoracic Society and European Respiratory Society recommendations. The solid lines are the model prediction of the end-exhalation C_{exh} at a constant exhalation flow rate using the mean value of the optimal parameter values determined from the flow rate maneuvers following 20-s breath hold.

niques, which require multiple-breathing maneuvers. Thus the technique has the potential to be applied to many different diseases and gather information on parameters that will likely provide more specific and sensitive information about NO metabolism and thus inflammation.

The backward integration of the flow signal (Eqs. 4 and 5) provides powerful flexibility, as a specific flow rate profile is not required. One requires knowledge of only the specific exhalation flow rate profile such that the backward integration is possible. Thus the method is very general and can be applied essentially to any given single exhalation profile. However, we utilized an exhalation maneuver with the following characteristics such that our model assumptions and simplifications were still valid, yet we were still able to accurately determine the unknown parameters: 1) the exhalation flow rate pattern produces exhaled boluses of gas with a wide range of uniformly distributed residence times to distinguish alveolar and airway contributions to exhaled NO (i.e., uniquely determine the three unknown parameters), 2) the rate of change in exhalation flow rate is small enough that each bolus of air resides for approximately the same amount of time in the different parts of the airways (i.e., minimal acceleration requirement, see DISCUSSION and APPENDIX below), and 3) easy to perform.

In agreement with the models described by Pietropaoli et al. (12) and Silkoff et al. (16), we assumed in this study that the linear dependence of J'_{NO} on C_{air} is constant along the airway tree. In fact, at any given axial position, the flux of NO will depend on many variables in addition to C_{air} such as tissue thickness, endogenous production and consumption rates, and airway diameter; thus the dependence of J'_{NO} on C_{air}

does not necessarily remain the same with axial position. Silkoff et al. (16) recently demonstrated that $D_{\text{NO,air}}$ for asthmatics was increased relative to healthy subjects even after treatment with corticosteroids. In an earlier study, Silkoff et al. (14) also reported that, in healthy lungs, a significant fraction of exhaled NO arises from the trachea ($\sim 45\%$), suggesting that the larger airways and mouth ($\sim 7\%$) were the primary sources of orally exhaled NO. This does not exclude the lower airways from contributing NO. In fact, the lower airways, together with the alveolar region, must account for the remaining $\sim 48\%$. Our model (as well as previous models) assumes that the contribution of NO from airways is evenly distributed

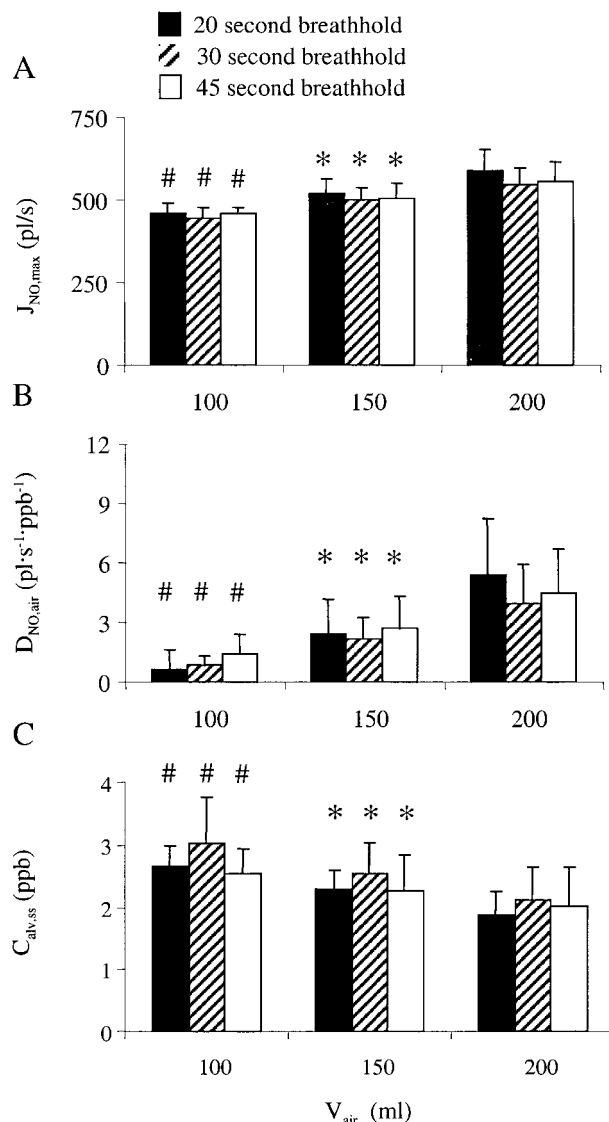


Fig. 8. The three estimated parameters [$J_{\text{NO,max}}$ (A), $D_{\text{NO,air}}$ (B), and $C_{\text{alv,ss}}$ (C)] are shown as a function of the choice for V_{air} for each of three breath-hold times (20, 30, and 45 s); 200 ml is the estimated value of the anatomic dead space for the subject based on the subjects ideal body weight in lb. plus the age in yr. *Statistically different from $V_{\text{air}} = 200$ ml. #Statistically different from $V_{\text{air}} = 150$ ml. Statistical significance was determined using a paired Student t -test and $P < 0.05$.

per unit airway volume. The volume of the trachea ($\sim 35\text{--}40$ ml) accounts for $\sim 20\text{--}25\%$ of the physiological dead space (V_{air}). Thus the larger airways are likely contributing a greater share per unit airway volume in healthy lungs, and the distribution of NO flux ($J_{\text{NO,max}}$ and $D_{\text{NO,air}}$) may change in disease states. This feature of NO exchange does not invalidate our governing equation but does place a requirement that the exhalation flow rate not change rapidly during the exhalation maneuver.

Rapid changes in the flow will result in significant acceleration (or deceleration) of a differential bolus of gas while traversing the airways. As a result, the bolus of gas will reside for different amounts of time in different parts of the airways, thus rendering our governing equation invalid. The APPENDIX predicts the maximum change in the flow rate during exhalation such that the residence time of any differential gas bolus not change by $>10\%$. Because we cannot preclude a nonuniform NO exchange distribution, such a flow profile minimizes the potential error in the estimation of $D_{\text{NO,air}}$ and $J_{\text{NO,max}}$.

Our sensitivity analysis (Fig. 3) demonstrates that a range of flow rates (or residence times) is necessary to uniquely determine the three parameters. This can be understood if one considers the limiting cases. At very high flow rates, the residence time in the airway compartment approaches zero, and thus very little NO is absorbed by the exhalate. Thus the exhaled NO concentration approaches that of $C_{\text{alv,ss}}$. The sensitivity is therefore highest for $C_{\text{alv,ss}}$ at very small airway compartment residence times; however, very little information can be extracted about the airway compartment. Conversely, as the residence time increases, a progressively increasing proportion of the exhaled NO is derived from the airway compartment; thus the parameters that characterize the airway compartment ($J_{\text{NO,max}}$ and $D_{\text{NO,air}}$) can be uniquely determined.

To estimate $D_{\text{NO,air}}$, much longer residence times are necessary. This is observed in Fig. 3 and can be explained by Eq. 3. $D_{\text{NO,air}}$ only becomes significant (or impacts J_{NO}) when C_{air} is large enough such that the second term in Eq. 3 becomes significant. Thus the exhalation flow rate must be low such that NO can accumulate in the airways. This increases C_{air} and decreases the driving force for diffusion of NO in the airstream. One choice in handling this problem is to increase the flow rate range by including smaller flows (higher residence times). Pietropaoli et al (12) and Silkoff et al (16) utilized flows less than 10 ml/s to accomplish estimation of $D_{\text{NO,air}}$. Alternatively, we utilized a preexpiratory breath hold (limit of zero exhalation flow rate) to achieve long residence times. We believe this alternative provides equivalent information about the airway compartment and is more easily performed by the subject, as well as more easily recorded by the investigator.

An exhalation that spans a wide range of flows may not however be sufficient unless each flow is sustained for a sufficient time to allow a bolus of air to traverse the airways at a specific flow rate. For example a 10

ml/s flow rate in a 150-ml airway will result in an exhaled bolus of gas with a residence time of 15 s. Thus, to characterize the concentration of such a bolus, the flow rate should be sustained for at least 15 s. In a single-exhalation maneuver with a dynamically changing flow rate, lower flows should be sustained for more time than high flows to collect exhaled concentrations that accurately span a wide range of residence times. Ideally, the residence time should also be distributed uniformly over this wide range such as to acquire the same amount of data at any given residence time.

On the basis of the above specifications, we propose a single-exhalation maneuver that includes a preexpiratory breath-hold time, followed by a flow rate pattern that decreases approximately exponentially with volume (see APPENDIX) from $\sim 6\%$ of the VC per second (300 ml/s in our subjects) to $\sim 1\%$ of the VC per second (50 ml/s in our subjects). Such a pattern provides exhaled boluses of gas whose flow rates do not change significantly during their passage through the airways (difference of entering to exiting velocity $<10\%$, see APPENDIX). At the same time, the residence times of the exiting boluses are approximately uniformly distributed over a range between 0.5 and 3 s (see shaded area in Fig. 3). This provides the necessary sensitivity for the estimation of $C_{\text{alv,ss}}$ and $J_{\text{NO,max}}$.

The dependence of our parameter estimation on the choice of V_{air} presents a potential problem (Fig. 8). The dependence of the parameters, particularly $D_{\text{NO,air}}$, on V_{air} is because the model's prediction for the NO concentration in the airways during breath holding depends on the choice of V_{air} . For example, if V_{air} values decrease from 200 to 100 ml, the concentration in the airway compartment will increase more rapidly; thus, to predict the experimental concentration, $J_{\text{NO,max}}$ and $D_{\text{NO,air}}$ would need to decrease (Fig. 8).

However, the parameter most impacted by the choice of V_{air} is $D_{\text{NO,air}}$, which is determined primarily from the shape of the exhalation profile in phases I and II (or the breath hold). During a breath hold, the NO emitted into the airway compartment will disperse in either direction due to molecular diffusion and cardiac mixing. On the basis of a molecular diffusion coefficient of $0.27\text{ cm}^2/\text{s}$ for NO in the gas phase (4), a conservative length for dispersion during the breath hold is 2–4 cm. This axial distance is approximately equal to that between generations 6–15 based on Weibel's symmetric lung model (22). Thus axial dispersion will tend to create a shape for phases I and II similar to that generated if the NO flux was uniformly distributed, thus mitigating the impact of a nonuniform distribution in NO flux. Hence, even if the distribution of NO flux is altered in disease, the choice for V_{air} should not have a significant impact on the relative change in the parameter estimates due to disease.

Covariance analysis (Eq. 8) provides an a priori estimate (i.e., without the need of multiple maneuvers) for the accuracy of our predictions. Thus it can be utilized as a criterion for rejecting a profile or for specifying sufficient experimental conditions for parameter estimation (flow rate range, breath-hold time).

The covariance analysis suggests that a breath-hold time of 20 s in combination with the specific flow rate pattern are adequate for the specific subject in determining the parameters of interest. This theoretical prediction was validated by repeated measurements. Although a longer breath hold time may provide increased accuracy of the estimate of $D_{\text{NO,air}}$, the gain is minimal and the effort on the part of the patient increases dramatically. A 20-s breath hold may not be possible for those subjects with more advanced lung disease who are hypoxic or hypercarbic, and an alternative technique may be necessary. For example, further characterization of this technique in a given lung disease population may determine that $J_{\text{NO,max}}$ is as good an indicator of disease status as $D_{\text{NO,air}}$, and thus the breath hold may not be necessary in all patient populations. Additional studies on more normal subjects and those with inflammatory diseases are necessary before a formal recommendation can be made.

Although there was not a significant variation in the mean values of the parameters between *subjects 1* and *2*, there were differences in the confidence intervals. For *subject 2*, the intramaneuver confidence intervals were significantly larger than for *subject 1*. The intramaneuver confidence interval is a positive function of R_{LS} . Thus a large $\Delta \bar{I}_{0.95,i}^{\text{p}}$ reflects a large R_{LS} and, provided that the instrument error did not change between subject testing, can be considered an index of the accuracy or appropriateness of the two-compartment model. Thus there may be significant variation among the normal population in how well the two-compartment model can simulate NO exchange dynamics. In contrast, intrasubject confidence intervals for *subject 2* were very similar, or slightly improved, compared with *subject 1*. $\Delta \bar{I}_{0.95,i}^{\text{p}}$ is a positive function of the deviation of the estimate from the population mean (Eq. 12); thus it provides an index of the maneuver-to-maneuver reproducibility. Thus our naive subject (*subject 2*) was able to reproduce the breathing maneuvers to a similar degree as our experienced subject (*subject 1*). This finding suggests that the maneuver is relatively simple to perform and that patients from many subpopulations may be able to perform the maneuver with minimal training.

Recently, ATS provided recommendations for standardized procedures for the measurement of exhaled NO. They recommended a constant exhalation flow rate maneuver of 50 ml/s and recording of the NO plateau value. The flow rate should be maintained within 10% of this value throughout the exhalation. The recommendations acknowledged that theoretical predictions from our earlier work and others (12, 19) suggest that derivation of additional parameters of potential physiological importance, by analyzing the dependence of C_{exh} on \dot{V}_{E} , may be achievable.

The significance and utility of the parameters estimated in this study for identification and/or monitoring of inflammatory diseases need to be examined through extensive application of these methods. At this point, such experimental data are limited. Silkoff et al. (16) applied their method in asthmatic subjects with some

intriguing results. They found that $D_{\text{NO,air}}$ is fourfold higher in asthmatic patients and that this increase is independent of steroid treatment. In contrast, the NO plateau concentration does not change dramatically between normal subjects and asthmatic patients treated with steroids (9). Perhaps the most promising utility of this technique is to follow patients longitudinally and correlate intrasubject changes in these parameters with important clinical decisions such as therapeutic dose. Thus, if the same \dot{V}_{air} is used for a given subject over time [i.e., \dot{V}_{air} (ml) = subjects ideal body weight in lb. + age in yr], one should be able to accurately determine changes in NO exchange parameters over time. Finally, there are other techniques such as the single-exhalation CO_2 profile that might be used in conjunction with this technique as an independent assessment of physiological dead space.

An alternative method of describing the linear dependence of J'_{NO} on the bulk gas phase concentration is to utilize a mass transfer coefficient (or transfer factor) and a concentration difference (16)

$$J'_{\text{NO}} = \left(\frac{D_{\text{NO,air}}}{\dot{V}_{\text{air}}} \right) (\bar{C}_{\text{tiss,air}} - C_{\text{air}}) \quad (13)$$

where $\bar{C}_{\text{tiss,air}}$ is the mean (over radial position) concentration within the tissue phase and $D_{\text{NO,air}}$ is equivalent to a mass transfer coefficient or transfer factor. Mathematically, this representation of NO flux is equivalent to Eq. 3, in which $J_{\text{NO,max}} = D_{\text{NO,air}} \times \bar{C}_{\text{tiss,air}}$. Thus the airway compartment is now alternatively characterized by $D_{\text{NO,air}}$ and $\bar{C}_{\text{tiss,air}}$. We can estimate $\bar{C}_{\text{tiss,air}}$ by taking the ratio of $J_{\text{NO,max}}$ to $D_{\text{NO,air}}$. For *subject 1*, the mean values of $\bar{C}_{\text{tiss,air}}$ (with intermaneuver 95% confidence intervals) are 89 ppb (68%), 155 ppb (92%), 152 ppb (63%), and 144 ppb (64%) for 10-, 20-, 30-, and 45-s breath holds, respectively. One estimate from the 10-s breathing maneuver was discarded because it produced a large negative value that greatly skewed the estimate. For *subject 2*, the mean values of $\bar{C}_{\text{tiss,air}}$ (with intermaneuver 95% confidence intervals) are 85 ppb (124%), 112 ppb (26%), 133 ppb (28%), and 95 ppb (28%) for 10-, 20-, 30-, and 45-s breath holds, respectively. The variance of $\bar{C}_{\text{tiss,air}}$ is similar to the other three parameters, and the mean value does not depend strongly on breath-hold time. Although the mean values for the two subjects are similar to those recently predicted by Silkoff et al. (16), the variance of this data cannot be compared because they report only a intersubject variability for a technique that utilizes multiple-breathing maneuvers.

In conclusion, this study describes a new technique to characterize flow-independent parameters ($J_{\text{NO,max}}$, $D_{\text{NO,air}}$, and $C_{\text{alv,ss}}$), which can characterize NO exchange dynamics in the lungs. The maneuver entails appropriate analysis of only a single-exhalation breathing maneuver that should be tolerated by a wide range of subjects. In addition, our results suggest that the stringent requirements on the flow rate that ATS and ERS recommends are not needed. With proper analysis of a variable flow rate maneuver, one can

estimate flow-independent parameters that potentially provide more specificity and sensitivity to disease status. If necessary, one can then use the model to predict the NO plateau concentration at a constant flow (Fig. 7). This could be of importance, especially for young and diseased subjects that have difficulty sustaining a constant expiratory flow. Future studies must address intersubject variability and also must apply this technique in a variety of key populations, including healthy adults and children, and for inflammatory diseases such as bronchial asthma, chronic obstructive pulmonary disease, and cystic fibrosis before its true utility is characterized.

APPENDIX

To achieve an even distribution for the residence times sampled during an exhalation flow maneuver, one needs the $\tau_{\text{res}}(t)$ for any differential bolus of air to be a linear function of time. Thus it is easily demonstrated that, if the exhalation flow rate decreases exponentially with exhaled volume, one can achieve this linear dependence between $\tau_{\text{res}}(t)$ and t .

By specifying an exponentially decreasing \dot{V}_E with V and by using the relationship $\dot{V}_E = dV/dt$, one can establish the following relationship

$$\dot{V}_E = \dot{V}_{E0} e^{-cV} = 1/(\dot{V}_{E0}^{-1} + ct) \quad (A1)$$

where \dot{V}_{E0} is the initial flow rate and c is a linear multiplier. Any differential bolus entering at time t will reside in $\tau_{\text{res}}(t)$ such that the following relationship holds (similar to Eq. 5)

$$V_{\text{air}} = \int_t^{t + \tau_{\text{res}}(t)} \dot{V}_E dt \quad (A2)$$

One can then insert Eq. A1 into Eq. A2 and derive the following linear relationship between $\tau_{\text{res}}(t)$ and t

$$\tau_{\text{res}}(t) = (e^{cV_{\text{air}}} - 1)[(c\dot{V}_{E0})^{-1} + t] \quad (A3)$$

In addition, it follows from Eq. A1 that the ratio of exiting and entering velocities is the same for every differential bolus of gas

$$\frac{\dot{V}_E(t + \tau_{\text{res}})}{\dot{V}_E(t)} = e^{-cV_{\text{air}}} \quad (A4)$$

Thus the particular flow rate profile described by Eq. A1 provides the same relative change between the entering and exiting flow rates of any exhaled gas bolus. For our experiments, in which flow rate change is from ~ 300 to ~ 50 ml/s over a period of 15–20 s and 3–4 liters of exhaled volume, the approximate values of \dot{V}_{E0} and c are ~ 300 ml/s and ~ 0.50 liter $^{-1}$, respectively. Thus, from Eq. A4, the exiting velocity is $\sim 90\%$ of the entering velocity, thus providing support for the key assumption made in our governing equation as described in METHODS and in DISCUSSION.

This work was supported by National Heart, Lung, and Blood Institute Grant R29-HL-60636 and National Science Foundation Grant BES-9619340.

REFERENCES

1. **Alving K, Weitzberg E, and Lundberg JM.** Increased amount of nitric oxide in exhaled air of asthmatics. *Eur Respir J* 6: 1368–1370, 1993.
2. **Barnes PJ and Kharitonov SA.** Exhaled nitric oxide: a new lung function test. *Thorax* 51: 233–237, 1996.
3. **Beck JV and Arnold KJ.** *Parameter Estimation in Science and Engineering.* New York: Wiley, 1977.
4. **Bird RB, Stewart WE, and Lightfoot EN.** *Transport Phenomena.* New York: Wiley, 1960.
5. **Bouhuys A.** Respiratory dead space. In: *Handbook of Physiology. The Respiration.* Bethesda, MD: Am. Physiol. Soc., 1964, sect. 3, vol. 1, chapt. 27, p. 699–714.
6. **Gutierrez HH, Pitt BR, Schwarz M, Watkins SC, Lowenstein C, Caniggia I, Chumley P, and Freeman BA.** Pulmonary alveolar epithelial inducible NO synthase gene expression: regulation by inflammatory mediators. *Am J Physiol Lung Cell Mol Physiol* 268: L501–L508, 1995.
7. **Hyde RW, Geigel EJ, Olszowka AJ, Krasney JA, Forster RE, Utell MJ, and Frampton MW.** Determination of production of nitric oxide by lower airways—theory. *J Appl Physiol* 82: 1290–1296, 1997.
8. **Kharitonov S, Alving K, and Barnes PJ.** Exhaled and nasal nitric oxide measurements: recommendations. The European Respiratory Society Task Force. *Eur Respir J* 10: 1683–1693, 1997.
9. **Kharitonov SA, Yates D, Robbins RA, Logan-Sinclair R, Shinebourne EA, and Barnes PJ.** Increased nitric oxide in exhaled air of asthmatic patients. *Lancet* 343: 133–135, 1994.
10. **Kimberly B, Nejadnik B, Giraud GD, and Holden WE.** Nasal contribution to exhaled nitric oxide at rest and during breathholding in humans. *Am J Respir Crit Care Med* 153: 829–836, 1996.
11. **Lehtimaki L, Turjanmaa V, Kankaanranta H, Saarelainen S, Hahtola P, and Moilanen E.** Increased bronchial nitric oxide production in patients with asthma measured with a novel method of different exhalation flow rates. *Ann Med* 32: 417–423, 2000.
12. **Pietropaoli AP, Perillo IB, Torres A, Perkins PT, Frasier LM, Utell MJ, Frampton MW, and Hyde RW.** Simultaneous measurement of nitric oxide production by conducting and alveolar airways of humans. *J Appl Physiol* 87: 1532–1542, 1999.
13. **Shaul PW, North AJ, Wu LC, Wells LB, Brannon TS, Lau KS, Michel T, Margraf LR, and Star RA.** Endothelial nitric oxide synthase is expressed in cultured human bronchiolar epithelium. *J Clin Invest* 94: 2231–2236, 1994.
14. **Silkoff PE, McClean PA, Caramori M, Slutsky AS, and Zamel N.** A significant proportion of exhaled nitric oxide arises in large airways in normal subjects. *Respir Physiol* 113: 33–38, 1998.
15. **Silkoff PE, McClean PA, Slutsky AS, Furlott HG, Hoffstein E, Wakita S, Chapman KR, Szalai JP, and Zamel N.** Marked flow-dependence of exhaled nitric oxide using a new technique to exclude nasal nitric oxide. *Am J Respir Crit Care Med* 155: 260–267, 1997.
16. **Silkoff PE, Sylvester JT, Zamel N, and Permutt S.** Airway nitric oxide diffusion in asthma. Role in pulmonary function and bronchial responsiveness. *Am J Respir Crit Care Med* 161: 1218–1228, 2000.
17. **Slutsky AS and Drazen JM.** Recommendations for standardized procedures for the online and offline measurement of exhaled lower respiratory nitric oxide and nasal nitric oxide in adults and children 1999. *Am J Respir Crit Care Med* 160: 2104–2117, 1999.
18. **Su W-Y, Day BJ, Kang B-H, Crapo JD, Huang Y-CT, and Chang L-Y.** Lung epithelial cell-released nitric oxide protects against PMN-mediated cell injury. *Am J Physiol Lung Cell Mol Physiol* 271: L581–L586, 1996.
19. **Tsoukias NM and George SC.** A two-compartment model of pulmonary nitric oxide exchange dynamics. *J Appl Physiol* 85: 653–666, 1998.
20. **Tsoukias NM, Tannous Z, Wilson AF, and George SC.** Single-exhalation profiles of NO and CO₂ in humans: effect of dynamically changing flow rate. *J Appl Physiol* 85: 642–652, 1998.
21. **Watkins DN, Peroni DJ, Basclain KA, Garlepp MJ, and Thompson PJ.** Expression and activity of nitric oxide synthases in human airway epithelium. *Am J Respir Cell Mol Biol* 16: 629–639, 1997.
22. **Weibel E.** *Morphometry of the Human Lung.* New York: Springer-Verlag, 1963.